
METHODS

Erythrocyte Membrane Surface after Calibrated Electroporation: Visualization by Atomic Force Microscopy

A. M. Chernysh*, E. K. Kozlova*, V. V. Moroz,
P. Yu. Borshagovskaya, U. A. Bliznuk, and R. M. Rysaeva

Translated from *Byulleten' Eksperimental'noi Biologii i Meditsiny*, Vol. 148, No. 9, pp. 347-352, September, 2009
Original article submitted July 1, 2008

Atomic force microscopy was used for examination of the surface of human erythrocyte membrane after calibrated electroporation and application of pharmacological agents. Three-order surface inhomogeneities were revealed with various spectral windows of Fourier transform to elaborate the quantitative criteria to assess the state of membrane surface. The size of structural alterations induced in the membranes by electroporation was 100-300 nm, which is comparable to the size of membrane matrix.

Key Words: *erythrocyte membrane; electroporation; atomic-force microscopy*

Electroporation results from the action of pulsed field on the cell membrane. This phenomenon accompanies defibrillation of the heart [5,13] and is used for drug delivery into the cell [8,10] and to assess membrane status [2,3,12]. Electroporation is observed in cells exposed to external electric field of high intensity. If the induced transmembrane potential φ surpasses a certain threshold value of $\varphi_{\text{thresh}} = 400\text{--}600$ mV, it produces electrical breakdown of the membrane yielding the pores. Depending on the value of induced potential φ , this breakdown can be reversible, so the pores resealed spontaneously in a short period of time (1-10 μsec). Reversibility of membrane breakdown occurs under the following condition: $\varphi \leq (1.5\text{--}2.0) \varphi_{\text{thresh}}$. Such reversible electroporation is used in clinics. However, irreversible

electroporation can appear during electrical defibrillation and in diagnostics of erythrocytes.

The electrical breakdown does not appear on the entire surface of the membrane. Initially, it originates at the local membrane defects [1,7]. However, it is difficult to observe this initial stage of the membrane breakdown experimentally.

At present, examination of the surface of biological objects is carried out with scanning contact microscopy, atomic force microscopy included (AFM) [6,9,14]. Although AFM can efficiently visualize the membrane surface ranging from dozens of microns to few nanometers, it faces pronounced difficulties in solving some problems, because analysis of complicated inhomogeneous surfaces of biological membranes is problematic. The obtained results cannot be adequately interpreted due to the lack of universal approaches for the analysis of these surfaces [9,11].

Our aim was to elaborate quantitative informative method for the analysis of the surface of erythrocyte membrane before and after the calibrated electroporation.

Research Institute of General Resuscitation Russian Academy of Medical Sciences, Moscow; I. M. Sechenov Moscow Medical Academy, Russia. **Address for correspondence:** amchernysh. A. M. Chernysh

MATERIALS AND METHODS

Experiments were carried out on the whole human venous blood stabilized with heparin (1 U per 1 ml blood). The donor was a practically healthy man (a physician) aged 26 years. Thirty minutes after drawing, 1.4 ml blood was placed into a quartz cuvette with titanium electrodes and exposed to pulsed electric field with intensity and pulse duration of 1700 V/cm and 9 msec, respectively. During electric shock, blood temperature was 19°C. The induced transmembrane potential ϕ was 450-560 mV depending on design of the cuvette. A Lifepak-7 clinical defibrillator was used as a generator of pulsed electric field. The details of calibrated electroporation technique are described elsewhere [1,4].

Before and after application of the electric pulse, the blood specimens were placed on a matrix to form erythrocyte monolayer, which was then dried on air at room temperature. The specimens formed before electroporation were used as the control.

Another method to prepare the specimens was also used. The blood cells were fixed in 1% glutaraldehyde, centrifuged at 5000 rpm, and washed in distilled water. Glutaraldehyde bound membrane proteins and disturbed membrane microstructure resulting in distortion of the results of comparative analysis of the examined surface. Moreover, a certain amount of hemoglobin leaked from cells after electroporation due to osmotic hemolysis and bound with glutaraldehyde. As a result, the solution solidified, so centrifugation, washing, and isolation of erythrocytes were significantly impeded.

However, glutaraldehyde was indispensable to wash the salts after processing of the erythrocyte suspension in buffer solution, otherwise it would be impossible to obtain image in AFM due to clogging of the cells.

The images of membrane surface were formed in the continuous scanning mode of a Femtoscan AFM with the use of its applied software. Standard fp N10 cantilevers with tip angle $\leq 22^\circ$ and approximate radius of ~ 10 nm were employed as the probes. During scanning, the applied force ranged 1.0-45 nN. The number of scanned points was 512, and these points were distributed within the following image fields: $10 \times 10 \mu$, 1500×1500 nm, 800×800 nm, and 50×50 nm.

The fragment of control membrane in the initial image (1500×1500 nm) was a complex uneven surface, whose profile was characterized by spatial periods T1-3 and heights h1-3 of the depressions and eminences (Fig. 1, a). The corresponding parameters greatly differed, but at the same time, they were characteristic of the particular membrane surface fragment of the erythrocytes. The comparison of the roughness parameters (Fig. 1, a) of the sur-

face of control cells and the cells exposed to various physicochemical stimuli cannot reveal significant and pronounced differences, because characteristic parameters T and h are intermixed (integrated) in calculation of the roughness parameters, so they become non-informative.

To obtain informative characteristics of the examined processes, we selected surfaces of three different orders from the initial surface (Fig. 1, a). To this end, we used spatial Fourier transform of the initial surface with three spectrum windows. The first order (I) of a surface corresponded to the spatial spectrum window with T_1 period in the range 1000-600 nm, while the II and III orders corresponded to $T_2=600-200$ nm and $T_3=200-50$ nm, respectively. The heights of depressions and eminences were not taken into consideration in the choice of the surface orders. They were measured in the experiments, which yielded the following ranges: $h_1=5-2$ nm, $h_2=2/1-0.8$ nm, and $h_3=0.90-0.24$ nm.

The surfaces resulted from mathematical processing of initial image (Fig. 1, a) are presented in 3D and profile plots of the individual orders: I order (Fig. 1, b), II order (Fig. 1, c) and III order (Fig. 1, d). Both profiles and 3D-images significantly differ, although on the whole, they represent various components of the same initial surface (Fig. 1, a). Summation of all three profiles and all three surfaces yielded the initial profile (Fig. 1, a) and initial image of the surface. In the following, we analyze the effect of pulsed electric field on the cells and compare the surfaces of the same orders for the control and experimental (exposed to the field) membranes.

In total, 12 experiments with electroporation of erythrocytes were carried out. In each experiment, three images of the cells were scanned in the field of $10 \times 10 \mu$. Then, three fragments were scanned for each cell in the field of 1500×1500 nm. These images were used to further scan the fields of 1000×1000 nm and 500×500 nm. As a result, 564 images were obtained and analyzed.

RESULTS

The plane images are presented in the field of 1500×1500 nm for the first- and second-order surfaces, while the third-order surfaces are shown in the field of 1000×1000 nm. The histograms of the periods and statistical parameters for the heights of surface inhomogeneities are given for all the images.

Shown are the first-order surfaces for the control (Fig. 2, a) and experimental (Fig. 2, b) membranes exposed to the pulsed field.

The mean values of the periods over the image assembly were: $T_1=813 \pm 360$ nm in the control and $T_1=710 \pm 100$ nm after electric shock. Similarly, the

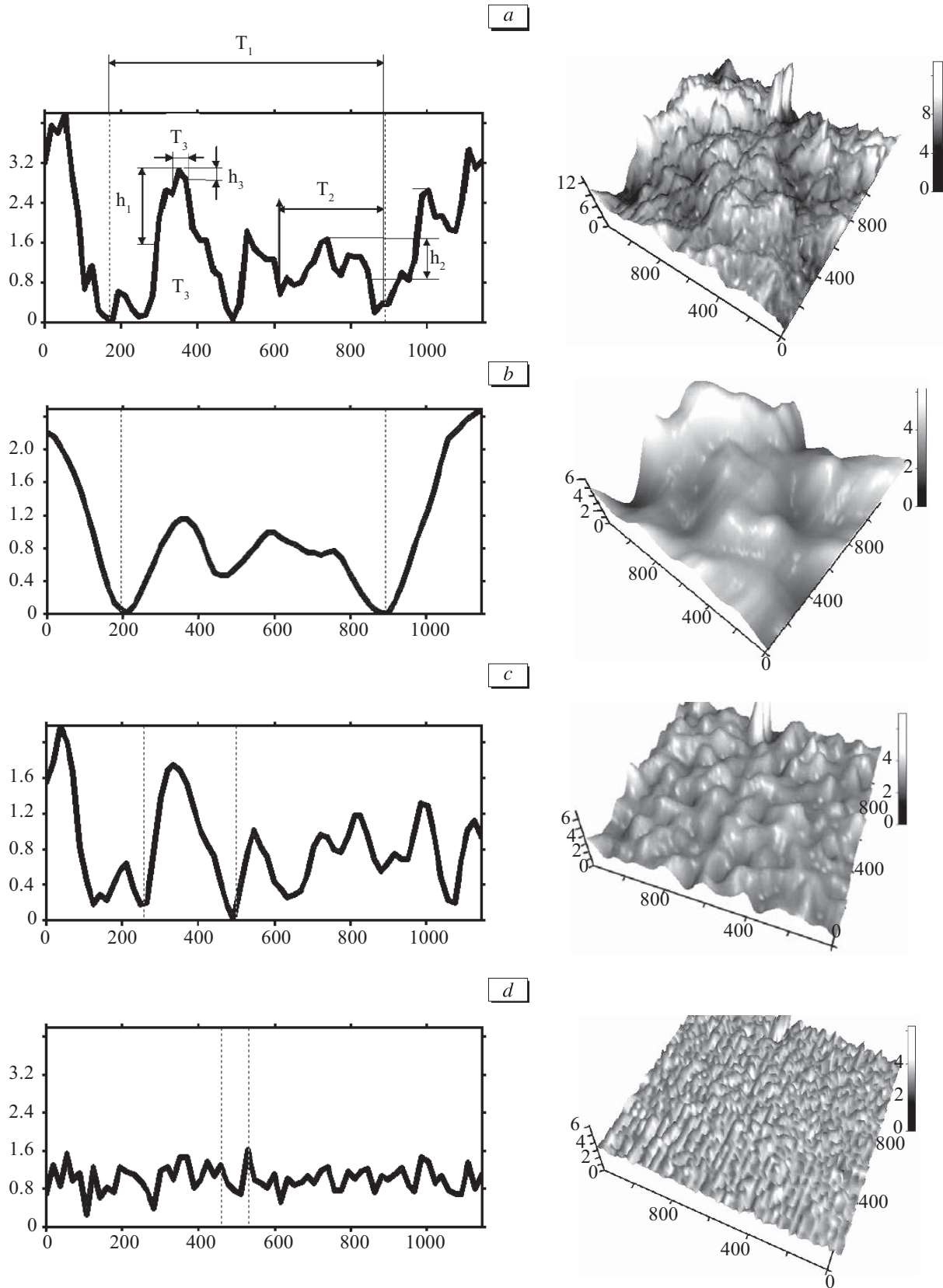


Fig. 1. 3D images and profiles of a fragment of erythrocyte membrane surface. *a*) initial image; *b*) first-order image, *c*) second-order image; *d*) third-order image.

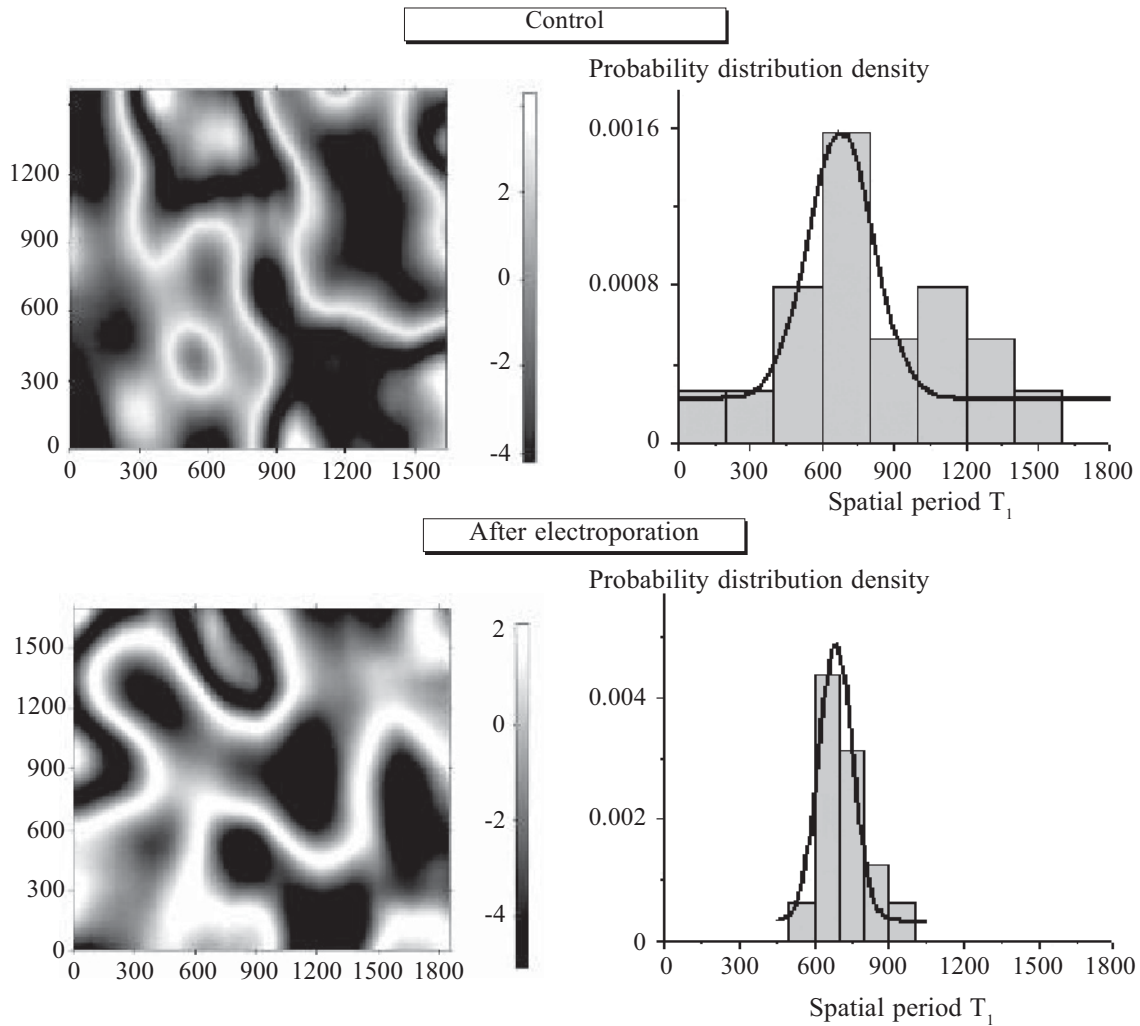


Fig. 2. The first-order images of the erythrocyte membranes.

control and experimental values for the heights were $h_1=2.28\pm 0.96$ nm and $h_1=2.65\pm 0.95$ nm, respectively. There were no significant differences between the control and experimental values for periods and heights.

Figure 3 shows the second- and third-order surfaces. In surface assembly, the mean values of the second-order periods and heights before and after electroporation (in brackets) were as follows: $T_2=300\pm 110$ nm (213 ± 72 nm) and $h_2=1.0\pm 0.5$ nm (1.1 ± 0.6 nm). The control and experimental periods differed significantly ($p<0.01$). In contrast, there were no significant differences between the control and experimental heights.

The mean values of the third-order periods and heights before and after electroporation (in brackets) were as follows: $T_3=104\pm 34$ nm (75 ± 18 nm) and $h_3=0.4\pm 0.2$ nm (0.5 ± 0.3 nm). The differences were significant both for periods ($p<0.01$) and heights ($p<0.04$).

Even visual inspection of initial images of erythrocyte surface (Fig. 1, a) showed that these surfaces

were inhomogeneous, and their roughness differed in various parts of the image.

In various cell ($n=12$), the control first-order surfaces did not practically differ. The same was true for the second- and the third-order surfaces. Thus, the surfaces of the same order did not significantly differ in the control.

Comparison of the control and experimental membranes (exposed to calibrated electroporation) revealed no changes in the first-order surfaces. The second-order surfaces differed in periods, which became significantly smaller after electroporation. Electroporation significantly modified the third-order surfaces: their periods decreased, while the height increased.

Thus, electroporation induced the structural alterations in erythrocyte membrane at the characteristic size of 100-300 nm. This range corresponds to the size of structures in spectrin matrix [14]. It can be hypothesized that electroporation induces conformational rearrangements in membrane cytoskeleton. However,

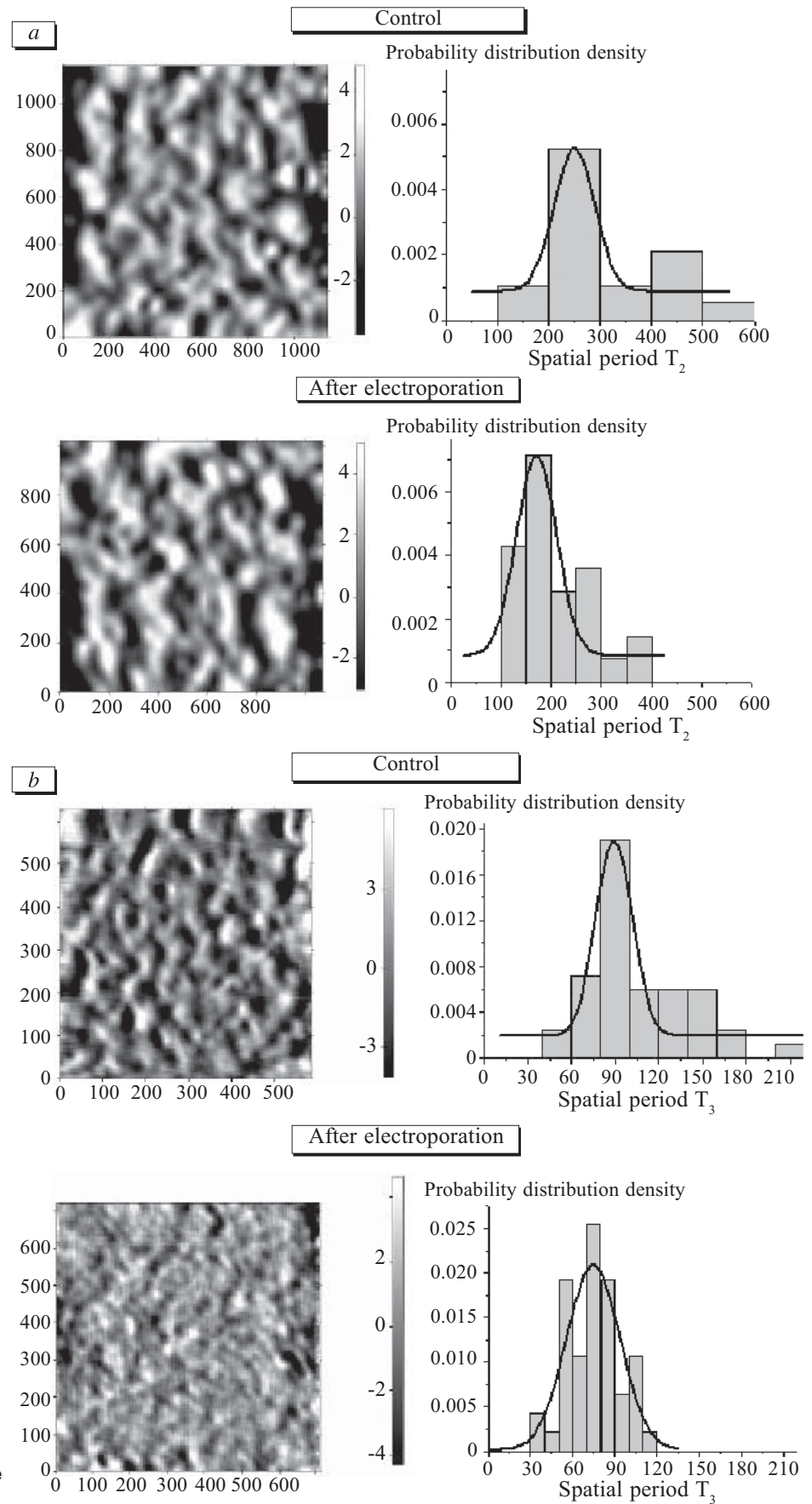


Fig. 3. The fragments of membrane surfaces of II (a) and III (b) orders.

further work is needed to substantiate this speculation. Our data agree with previous reported [9,11,14].

Therefore, presentation of initial membrane surface by inhomogeneities of three orders yielded quantitative criteria to compare the state of the membranes and to reveal significant differences in the structure of human erythrocyte membrane surface prior and after electroporation.

The method of AFM combined with decomposition of initial image of membrane surface into the spectrum components can be used to compare the surfaces after some other physicochemical stimulation and to assess the effect of therapeutic preparations on the erythrocytes.

REFERENCES

1. P. Yu. Alekseeva, U. A. Bliznuk, V. M. Elagina, *et al.*, *Obshch. Reanimatol.*, **3**, No. 4, 18-23 (2007).
 2. V. V. Moroz, A. M. Chernysh, M. S. Bogushevich, *et al.*, *Byull. Eksp. Biol. Med.*, **137**, No. 2, 141-144 (2004).
 3. A. M. Chernysh, E. K. Kozlova, V. V. Moroz, *et al.*, *A Method to Reveal Membrane Damage* [in Russian], Patent RF No. 2269127 (2004).
 4. A. P. Chernyaev, A. M. Chernysh, P. Yu. Alekseeva, *et al.*, *Tekhnol. Zhiv. Sist.*, **4**, No. 1, 28-37 (2007).
 5. A. Al-Khadra, V. Nikolski, and I. R. Efimov, *Circ. Res.* **87**, No. 9, 797-804 (2000).
 6. T. Betz, U. Bakowsky, M. Müller, *et al.*, *Bioelectrochemistry*, **70**, No. 1, 122-126 (2007).
 7. K. A. DeBruin and W. Krassowska, *Biophys. J.*, **77**, No. 3, 1213-1224 (1999).
 8. J. Gehl, *Acta Physiol. Scand.*, **177**, No. 4, 437-447 (2003).
 9. M. Girasole, G. Pompeo, A. Cricenti, *et al.*, *Biochim. Biophys. Acta*, **1768**, No. 5, 1268-1276 (2007).
 10. M. Golzio, J. Teissie, and M. P. Rols, *Bioelectrochemistry*, **53**, No. 1, 25-34 (2001).
 11. T. Guha, K. Bhattacharyya, R. Bhar, *et al.*, *Cur. Sci.*, **83**, No. 6, 693-694 (2002).
 12. I. Petcu, D. Fologea and M. Radu, *Bioelectrochem. Bioenerg.*, **42**, 179-185 (1997).
 13. G. P. Walcott, C. R. Killingsworth and R. E. Ideker, *Resuscitation*, **59**, No. 1 59-70 (2003).
 14. S. Yamashina and O. Katsumata, *J. Electron. Microsc. (Tokyo)*, **49**, No. 3, 445-451 (2000).
-